

DEVELOPMENT OF QUALITY INDICATOR FOR STEREOSCOPIC PLOTTING USING ORIENTATION PARAMETERS OF UAV IMAGES

Pyung-Chae Lim (1), Hae-Min Lee (1), Yeong-Min Cho(1), Jung-Il Shin (2), Taejung Kim (1), Suk Bae Lee (3)

¹ Department of Geoinformatic Engineering, Inha Univ., 100 Inha-ro, Michuhol-gu, Incheon, Korea

² Geoinformatic Engineering Research Center, Inha Univ., 100 Inha-ro, Michuhol-gu, Incheon, Korea

³ Department of Civil Engineering, Gyeongnam National Univ. of Science and Technology, 33 Dongjin-ro, Jinju, Gyeongsangnam-do, Korea

Email: vudco88@inha.edu, 12161136@inha.edu, 12131075@inha.edu, jishin@inha.ac.kr,
tezid@inha.ac.kr, sblee@gntech.ac.kr

KEY WORDS: UAV mapping, large scale digital map, Y-parallax, Absolute-Model Accuracy, stereoscopic plotting

ABSTRACT: An unmanned aerial vehicle (UAV) acquires images at higher spatial resolution than airplanes or satellites. It opens a possibility for large scale digital map generation at low cost. Recently, studies are being conducted to generate large scale maps using UAVs. Most of researcher are using UAV commercial software such as Pix4D and PhotoScan. While they provide information such as camera calibration and bundle adjustment quality, they do not provide any quality indicators for a large scale digital map generation. In this paper, we develop a technique to indicate the quality to generate a large scale digital map by calculating the quality of stereoscopic plotting. We aim to utilize interior and exterior orientation parameters and tie-points derived from UAV images and to exclude the use of ground control points. For measuring this quality, we propose to use check-points to calculate Y-parallax and absolute-model accuracy among the adjacent stereo models. The Y-parallax affects the quality of stereo-viewing and hence the possibility of stereo-plotting using the images. The absolute model accuracy affects stereoscopic plotting accuracy for digital mapping. The absolute model accuracy can be calculated by the difference of object coordinates at check-points observable in several stereo models. We compared UAV images processed from various UAV SW with the quality of stereoscopic plotting by using orientation parameters. The analysis results showed that the rotary-wing produced the quality of stereoscopic plotting that was more accurate than the fixed-wing. By using this technique, we can conclude that large scale digital map accuracy can be predicted in advance.

1 INTRODUCTION

UAVs began with research and development for military use. Recently, as the UAV range is rapidly expanded for industrial and private use, they are used in various fields such as precision agriculture, change detection and mapping. The Association for Unmanned Vehicle Systems International predicts that UAV market of the 82 billion dollars will be formed in the United States from 2015 to 2024, and new jobs will be created through this market. A UAV requires platform design technology, on-board sensor technology, system integration technology, communication technology, etc. UAV industry is a high value-added industry with various applications and high utilization.

UAVs whose main purpose is to obtain and provide image information are equipped with Electro Optical (EO) and Infrared (IR) sensors. Sensors for image information require various resolutions depending on the observation purpose and operation method.

The UAV equipped with EO sensors for mapping captures images at a lower altitude than aircraft and satellite, so that high quality images with high resolution can be obtained. Above all, there is an advantage that it can acquire images frequently because there are no big restrictions on operation and flight. These advantages make the mapping industry very interested in the possibility of 1: 1,000 scale mapping using UAVs.

UAVs are more difficult to acquire orthoimages than conventional aircraft due to unstable flight posture and low altitude imaging. UAVs can be classified into fixed and rotary wings according to their flight characteristics. The fixed-wing is useful for shooting a large area because it can fly at high speed and long time, but it is difficult to mount gimbal in structure and acquires unstable orientation. On the other hand, the rotary-wing can be gimbal mounted so that stable orientation and high redundancy images can be acquired (Son *et al.*, 2019).

Because of the UAV's ability to acquire images at low altitudes, hundreds of multiple images are required to map the region of interest. 3D mapping takes a lot of time and labor. Therefore, it is necessary to select only high

quality stereo models from all pairs. Currently, UAV image processing software provides camera calibration or bundle adjustment accuracy quality but does not provide the quality of stereoscopic plotting for digital mapping. Therefore, in this study, we developed a technique to calculate the Y-parallax and absolute model accuracy for generating the quality of stereoscopic plotting by using the orientation parameters from the UAV image processing software.

2. EXPERIMENTAL SET-UP

2.1 Study area and UAV platforms

The research area photographed region of 0.5 km² in the urban area consisting of buildings and roads. In order to evaluate the precise quality of stereoscopic plotting, a total of 19 ground control points (GCPs) were surveyed, consisting of 8 model points and 11 check points. The fixed-wing was an eBee manufactured by Sensfly, equipped with an S.O.D.A camera, and the rotary-wing was an Inspire 2 manufactured by DJI, with a gimbal and Zenmuse X5S.

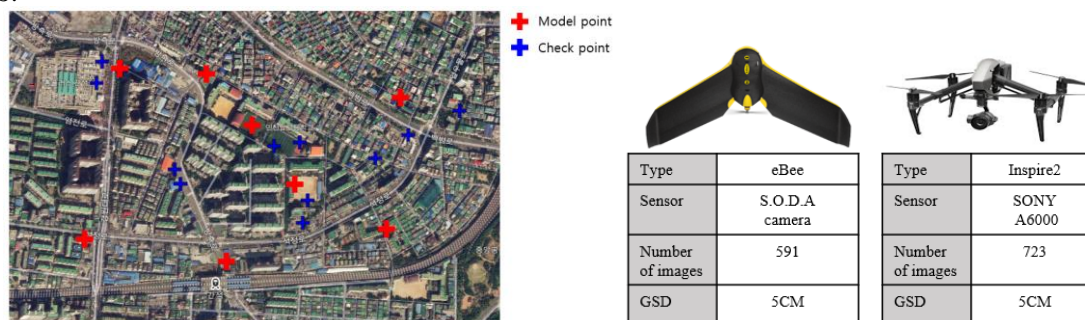


Figure 1. Study area with GCPs (left) and the used UAV platforms (right)

2.2 Used software

We used two different types of software Pix4DMapper and 3D-UAV for extracting orientation parameters. Pix4DMapper is most popular UAV image processing software in the world. For the 3D-UAV developed in house, is an incremental bundle adjustment algorithm based on photogrammetry that produces precise automatic exterior orientation parameters capable of digital mapping. We performed a previous study that compared DSM and height accuracy using 3D-UAV and Pix4DMapper (Lim and Kim., 2018).

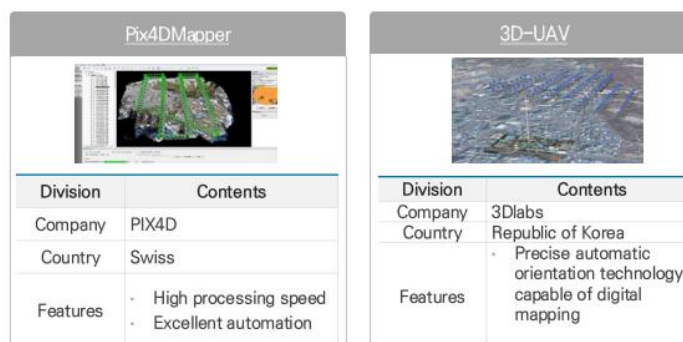


Figure 2. UAV image processing software types and features

3. METHODOLOGY

3.1 Camera calibration using open software

The camera calibration is the process of determining the camera's focal length, principal point, and lens distortion coefficients (Kim *et al.*, 2010). Conventional survey metric cameras for mapping are very expensive precision sensors with precisely calculated focal lengths and principal point and very small lens distortion coefficients (Lim *et al.*, 2019a). On the other hand, a camera equipped with an UAV requires a self-calibration because it is equipped with a non-mapping camera (Won *et al.*, 2012). Using distorted images in mapping can have a big impact on mapping accuracy. The calibration was performed through the open SW Camera Calibration Toolbox for Matlab. The open SW has been used in many studies as a representative open SW in the field of camera calibration (Fetić *et al.*, 2012). We used this SW in our previous study to calculate interior orientation parameters (Lim *et al.*, 2019b). The camera calibration process using the open SW is as follows. First, shoot the chess board in various directions and select the corner points of the chess board. After selecting the 1st automatic edge point, check the edge point selection result. If calibration is needed, enter manual radial distortion to correct the edge point. The corner point selection error, which was manually selected, was corrected to produce a more accurate final calibration result.

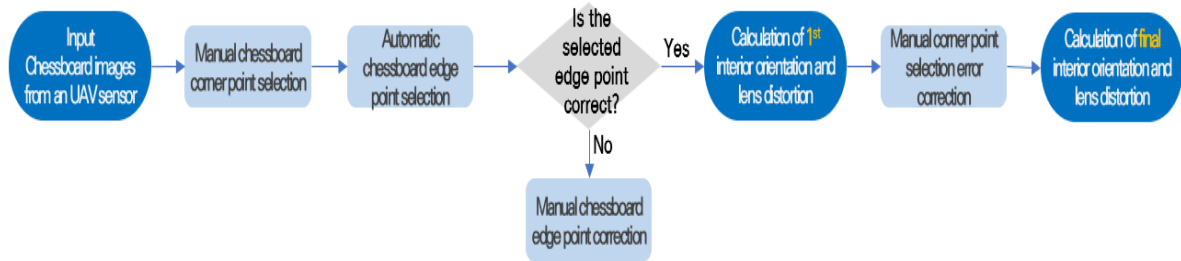


Figure 3. Camera calibration process using Camera Calibration Toolbox for Matlab

3.2 Extracting orientation parameters from software

The interior and exterior orientation parameters were calculated by using each software. As mentioned in Section 3.1, the interior orientation parameters include the focal length, principal point and the lens distortion coefficient which are corrected through the camera calibration process. The exterior orientation parameters are calculated from the GPS / IMU sensor equipped with the UAV and include the position and orientation information of the captured image. The initial exterior orientation parameters obtained from the UAV are updated by precise exterior orientation parameters through the process of precise bundle adjustment.

The process of calculating the precision exterior orientation parameters are largely four steps, which requires initial tie-points extraction, camera calibration, distortion-corrected tie-points update and precision bundle adjustment process using model points. The first step is to extract the tie- points from the original image. In the second step, interior orientation parameters are calculated through camera calibration. General commercial software calculates interior orientation parameters using the tie-points. In this study, precise interior orientation parameters were calculated using the Camera Calibration Toolbox for Matlab. In the third step, the initial tie-points must be updated with the corrected tie points using interior orientation parameters. Using initial tie-points in the original image with distortion affects the mapping accuracy, so it must be updated with corrected tie-points. In the fourth step, precise bundle adjustment is performed using the calibrated tie-points and the model- points.

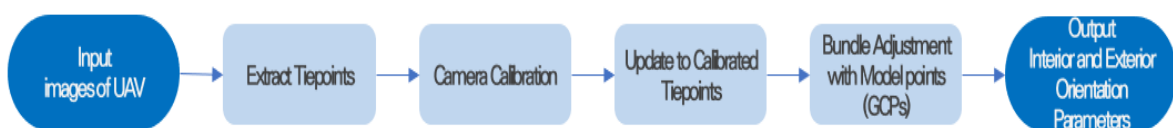


Figure 4. UAV image processing to generate orientation parameters

3.3 Calculating Y-parallax and Absolute-Model Accuracy

The quality of stereoscopic plotting can be predicted by the Y-parallax and absolute model accuracy using orientation parameters. If the Y-parallax increase, stereo-viewing is difficult, 3D digital mapping is impossible or fatigue occurs to the operator. The epipolar geometry can be constructed using the orientation parameters of the image and the accuracy of the Y-parallax can be calculated through the epipolar line. Epipolar geometry means that the projection centers (O, O') of two images, a point P in 3D space and (p, p') projected on each image exist on a common plane. At this time, the point where the line segment connecting the two projection centers meets each image plane is called epipole. Theoretically all epipolar lines of the image converge at epipole. When the point P in 3D space is projected as point p on the image plane of A, the epipolar line is the curve l' that appears when the straight line connecting them is projected on the other image B (Figure 5). In the central projection camera, the curve appears as a straight line (Kim and Kim., 2012). Y-parallax can be calculated by applying epipolar resampling using the orientation parameters and checking the difference of y coordinates between stereo pairs at the same locations.

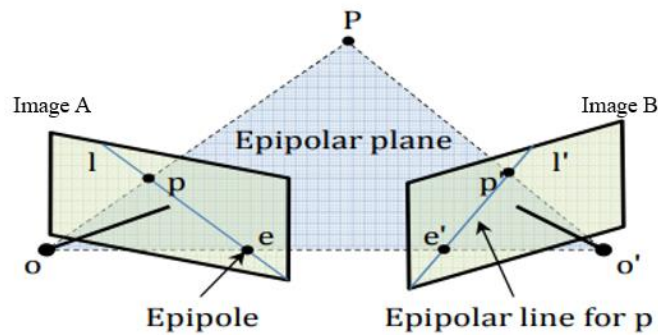


Figure 5. Epipole and epipolar line at epipolar geometry (Kim and Kim., 2012)

The absolute model accuracy can be calculated from the difference between the object coordinates of the projected check-points on the image and the measured check-points. The several stereo models are composed by selecting images with common check-points visible. We can predict the absolute model accuracy by comparing the check-points with the same coordinate of $(X, Y, Z)^{pair}$ of the other stereo model (Figure 6).

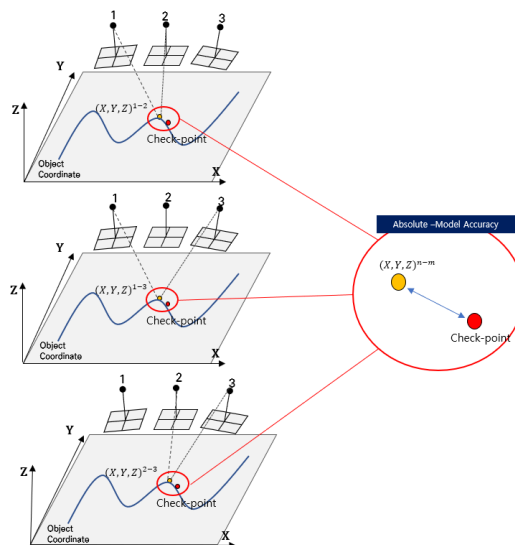


Figure 6. Absolute model accuracy using the check-point

The point (X_p, Y_p, Z_p) is a 3D position coordinate for a point P in space, the other point (X_o, Y_o, Z_o) is a center of the camera projection, s is a scale constant, r_{11} to r_{33} denotes a rotation matrix element for converting from camera space to real world space, x_p and y_p denote image coordinates and f denotes a camera focal length. The object coordinate P for a point p in the image can be calculated as Equation (1) through the collinearity condition equation.

$$\frac{X_p - X_o}{Z_p - Z_o} = \frac{r_{11}x_p + r_{12}y_p - r_{13}f}{r_{31}x_p + r_{32}y_p - r_{33}f} \Rightarrow X_p = \frac{r_{11}x_p + r_{12}y_p - r_{13}f}{r_{31}x_p + r_{32}y_p - r_{33}f} (Z_p - Z_o) + X_o$$

$$\frac{Y_p - Y_o}{Z_p - Z_o} = \frac{r_{21}x_p + r_{22}y_p - r_{23}f}{r_{31}x_p + r_{32}y_p - r_{33}f} \Rightarrow Y_p = \frac{r_{21}x_p + r_{22}y_p - r_{23}f}{r_{31}x_p + r_{32}y_p - r_{33}f} (Z_p - Z_o) + Y_o \quad (1)$$

Z_p = reference height

3.4 Visual analysis using a Digital Photogrammetric Workstation (DPW)

We observed several stereo pairs on a DPW for generating the quality of stereoscopic plotting. We analyzed the possibility of stereo viewing by eyes directly and the absolute model accuracy by measuring check-points manually.

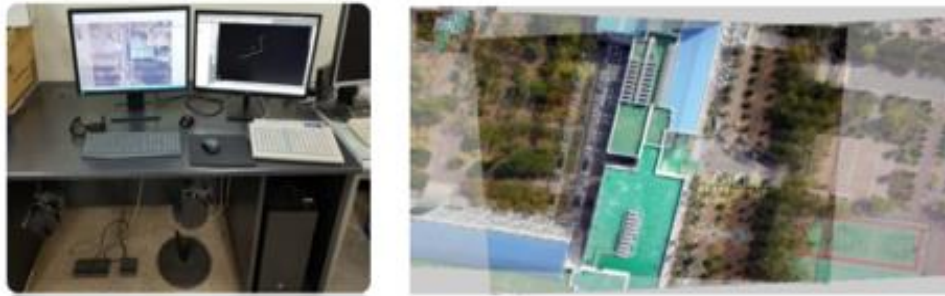


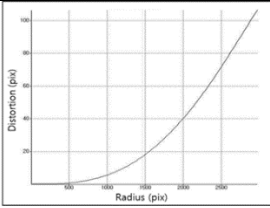
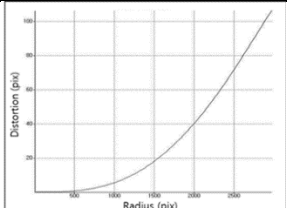
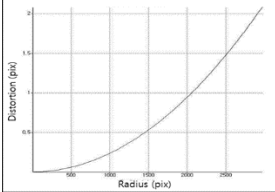
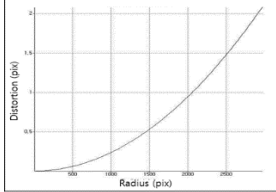
Figure 7. The DPW and stereo viewing (Lim *et al.*, 2019a)

4. RESULT AND DISCUSSION

4.1 Camera calibration result

Through the Camera Calibration Toolbox for Matlab, the camera lens distortion graphs and the interior orientation parameters were calculated as shown Table 1. The dPPx and dPPy mean the difference between the lens center coordinates and the principal point. In the radial and tangential distortion graph, as the radius increases, the radial and tangential distance increase all of cameras. These distortion graphs showed normal distortion characteristics of general cameras. In case of this SW, radial distortion coefficients were calculated only up to the K1 and K2. Rather, it may be reasonable not to apply K3 to distortion. Since the K3 is a six-squared coefficient of radius from the center of the image, it can have a sensitive effect to distortion. The tangential distortion is a distortion that occurs when the center of the lens and the sensor do not match in the camera manufacturing process. This distortion is generally negligible because close to zero as shown Table 1.

Table 1. Camera calibration results by UAV type

Type of Camera (Type of UAV)	S.O.D.A camera (eBee)	Zenmuse X5S (Inspire2)
Number of images for calibration	28	31
Image width (pixel)	5472	5472
Image Height (pixel)	3648	3648
Focal length (pixel)	4606.0774	3667.9466
Principle point x (pixel)	2727.6629	2741.9247
Principle point y (pixel)	1808.5404	1844.3532
dPPx: Center – PPx (pixel)	8.34 (0.15%)	5.95 (0.11%)
dPPy: Center – PPy (pixel)	15.46 (0.42%)	20.35 (0.56%)
Radial K1	-0.02707	0.0032
Radial K2	0.004344	-0.0016
Radial K3	0	0
Tangential T1	-0.0040	0.0082
Tangential T2	-0.0029	0.0013
Radial distortion graph		
Tangential distortion graph		

4.2 Stereoscopic plotting quality result

Five image pairs and check-points from each UAV (eBee and Inspire2) were selected to predict the Y-parallax. The ground coordinates of check points were measured by a digital photogrammetric workstation (DPW) manually and their accuracy was analyzed using the true ground coordinates of the check points. In Table 2, this accuracy is shown as ‘Absolute Model Accuracy from DPW’. For each image pair, predicted absolute model accuracy was analyzed and shown in Table 2 as ‘Predicted Absolute Model Accuracy’. The difference between these two accuracy was compared and shown as ‘Difference between DPW and Predicted’ in the table.

For the eBee, the Y-parallax of 3D-UAV and Pix4D were similar in all pairs. For the Pairs B and D, Y-parallax from the both SW were high while other pairs showed low Y-parallax. The Absolute-Model Accuracy using DPW showed that the 3D-UAV of the B pair showed the highest accuracy, and the Pix4D of the E pair showed the lowest accuracy. The horizontal error of the difference between Absolute-Model Accuracy from DPW and predicted Absolute-Model Accuracy in all pairs showed a range of error within 12 cm. On the other hand, the vertical error was greater than 1m in the D and E pairs. The A, C, and E pairs were considered to be stereo-viewable since the Y-parallax was less than 2 pixels (Lim *et al*, 2019b). However, when we actually observed image pairs using a DPW, stereo-viewing was almost impossible and stereo plotting was not possible. This phenomenon seemed due to unstable roll orientation among image pairs.

Table 2. The quality of stereoscopic plotting for eBee

Pair (GCP Index)	Type	Y-parallax (pixel)	Object Coordinate Accuracy From DPW (m)			Absolute-Model Accuracy From DPW (m)		Predicted Absolute-Model Accuracy (m)		Difference between DPW and Predicted (m)	
			x	y	z	Horizontal Error	Vertical Error	Horizontal Error	Vertical Error	Horizontal Error	Vertical Error
A (P2)	Check point	-	295712.700	4149475.720	42.928	-	-	-	-	-	-
	3D-UAV	1.070	295713.049	4149475.746	44.152	0.350	1.224	0.231	0.848	0.119	0.376
	PIX4D	1.240	295713.057	4149475.813	44.041	0.369	1.113	0.287	0.847	0.082	0.266
B (P6)	Check point	-	295918.424	4149238.240	29.393	-	-	-	-	-	-
	3D-UAV	3.720	295918.150	4149238.133	29.373	0.294	0.020	0.199	0.183	0.095	0.163
	PIX4D	3.140	295918.201	4149238.301	29.727	0.231	0.334	0.190	0.228	0.041	0.106
C (P7)	Check point	-	295932.552	4149199.050	29.249	-	-	-	-	-	-
	3D-UAV	1.210	295932.346	4149199.058	29.333	0.206	0.084	0.129	0.220	0.077	0.136
	PIX4D	1.260	295932.390	4149199.178	29.545	0.206	0.296	0.129	0.168	0.077	0.128
D (P15)	Check point	-	296260.803	4149085.960	30.103	-	-	-	-	-	-
	3D-UAV	5.600	296260.562	4149085.607	28.100	0.427	2.003	0.093	0.382	0.334	1.621
	PIX4D	4.550	296260.578	4149085.631	28.117	0.399	1.986	0.119	0.466	0.280	1.520
E (P20)	Check point	-	296461.286	4149255.010	28.840	-	-	-	-	-	-
	3D-UAV	1.750	296454.905	4149255.003	27.240	6.381	1.600	6.103	0.093	0.278	1.507
	PIX4D	1.710	296454.818	4149255.039	26.896	6.468	1.944	6.095	0.162	0.373	1.782

For Inspire2, the Y-parallax were estimated near zero in all pairs. As a result of Absolute-Model Accuracy using DPW, Pix4D of B and C pair showed the highest accuracy, and Pix4D of E pair showed the lowest accuracy. The horizontal and vertical error differences of Absolute-Model Accuracy and predictive Absolute-Model Accuracy of all pairs were between 14 cm and 30 cm. In particular, extremely accurate error ranges were predicted for B, C, and D pairs. Y-parallax was calculated to be close to zero in all pairs and stereo-viewing was very well formed when applied to DPW. This seemed that the Inspire2 was equipped with gimbals, and most of the images were captured close to true vertical images.

Table 3. The quality of stereoscopic plotting for Inspire2

Pair (GCP Index)	Type	Y-parallax (pixel)	Object Coordinate Accuracy From DPW (m)			Absolute-Model Accuracy From DPW (m)		Predicted Absolute-Model Accuracy (m)		Difference between DPW and Predicted (m)	
			x	y	z	Horizontal Error	Vertical Error	Horizontal Error	Vertical Error	Horizontal Error	Vertical Error
A (P2)	Check point	-	295712.700	4149475.720	42.928	-	-	-	-	-	-
	3D-UAV	0.290	295713.766	4149474.555	44.749	1.579	1.821	1.668	1.905	0.089	0.084
	PIX4D	0.230	295711.998	4149474.992	44.123	1.011	1.195	0.865	0.924	0.146	0.271
B (P6)	Check point	-	295918.424	4149238.240	29.393	-	-	-	-	-	-
	3D-UAV	1.540	295917.720	4149238.690	28.009	0.836	1.384	0.807	1.139	0.029	0.245
	PIX4D	1.120	295917.821	4149237.771	29.992	0.764	0.599	0.827	0.532	0.063	0.067
C (P7)	Check point	-	295932.552	4149199.050	29.249	-	-	-	-	-	-
	3D-UAV	0.650	295931.651	4149199.694	28.613	1.107	0.636	1.102	0.636	0.006	0.000
	PIX4D	0.400	295932.484	4149198.226	29.791	0.827	0.542	0.831	0.487	0.004	0.055
D (P15)	Check point	-	296260.803	4149085.960	30.103	-	-	-	-	-	-
	3D-UAV	0.510	296260.207	4149085.169	28.950	0.990	1.153	0.993	1.262	0.003	0.109
	PIX4D	0.450	296261.433	4149086.611	30.592	0.906	0.489	0.903	0.383	0.003	0.106
E (P20)	Check point	-	296461.286	4149255.010	28.840	-	-	-	-	-	-
	3D-UAV	0.410	296455.502	4149255.559	28.906	5.810	0.066	5.825	0.250	0.015	0.184
	PIX4D	0.430	296454.271	4149254.919	29.311	7.016	0.471	7.141	0.768	0.125	0.297

5. CONCLUSION

In this study, we developed a technique for predicting the quality of stereoscopic plotting before mapping using images taken from the UAVs and orientation parameters. For this, the Y-parallax was calculated using epipolar geometry, and the absolute accuracy was calculated by projecting image points into object space based on collinear conditional equation. As a result of applying fixed wing images with unstable orientation to a DPW, digital plotting was almost impossible due to the difficulty of stereo-viewing. The Y-parallax was largely calculated, and the error range of the prediction accuracy was also large. On the other hand, the rotary-wing images were well stereo-viewed in the DPW and digital plotting was possible. The Y-parallax was close to zero and predicted a low range of error. The absolute model accuracy estimated through the technique proposed here did not agree well with actual stereo measurement accuracy in the case of fixed-wing images. This seemed partly due to the difficulties of stereo viewing of the fixed-wing images tested. On the other hands, the proposed technique could generate the absolute model accuracy very close to actual stereo measurement accuracy in case of rotary-wing images with gimbal. Therefore, if the rotary-wing with a gimbal is used, the proposed technique is expected to save mapping time by selecting stereo images with high quality of stereoscopic plotting in advance.

ACKNOWLEDGEMENTS

This study was carried out with the support of "Cooperative Research Program for Agriculture Science & Technology Development (PJ01350003)" Rural Development Administration, Republic of Korea and with the support of "National Geographic Information Institute", Republic of Korea.

REFERENCES

P.C. Lim, and T. Kim, 2018. COMPARATIVE ANALYSIS OF POINT CLOUD GENERATION FROM UAV IMAGES USING VARIOUS COMMERCIAL AND PUBLIC SOFTWARE, International Symposium on Remote Sensing 2018, Digitally available on USB

G.H. Kim, J.H. Youn, and H.J. Park, 2010, The Accuracy of Stereo Digital Camera Photogrammetry, Journal of the Korean Society of Surveying, Geodesy, Photogrammetry, and Cartography, Vol.28, No 6, PP. 663-668

Won, J.H., So, J.K., and Yun, H.C., 2012, Non-Metric Digital Camera Lens Calibration Using Ground Control Points, Journal of the Korean Society of Surveying, Geodesy, Photogrammetry, and Cartography, Vol.30, No 2, PP. 173-180

A. Fetić, and Davor D. J. D. O, 2012, The procedure of a camera calibration using Camera Calibration Toolbox for MATLAB, MIPRO 2012

J. Leiner Barba, Q. Lorena Vargas, M. Cesar Torres, and V. Lorenzo Mattos, 2008, Three- Dimensional Reconstruction Optical System Using Shadow Triangulation, AIP Conference Proceedings 992, 1073 (2008); <https://doi.org/10.1063/1.2926793>

P.C. Lim, J. Seo, J. Son, and T. Kim, 2019a Feasibility Study for 1:1000 Scale Map Generation from various UAV images, International Symposium on Remote Sensing 2019, Digitally available on USB

P. C. Lim , J. Seo , J.Son , T. Kim, 2019b, ANALYSIS OF ORIENTATION ACCURACY OF AN UAV, The International Archives of the Photogrammetry, Remote Sensing and Spatial Information Sciences, Vol.XLII-2/W13, 2019

J. Son, P. Lim, J. Seo, and T. Kim, 2019, ANALYSIS OF BUNDLE ADJUSTMENTS AND EPIPOLAR MODEL ACCURACY ACCORDING TO FLIGHT PATH CHARACTERISTICS OF UAV, The International Archives of the Photogrammetry, Remote Sensing and Spatial Information Sciences, Vol.XLII-2/W13, 2019

J-I. Kim, and T. Kim, 2014, Automated Image Alignment and Monitoring Method for Efficient Stereoscopic 3D Contents Production, The Korean Society of Broadcast Engineers, Vol.19, No 2, pp. 205-214

Y. Tadjdhe, 2015, National Defense Magazine May 8, 2015, from <https://www.businessinsider.com/the-global-drone-market-is-booming-2015-5>